Crystallization Behavior of Poly(butylene succinate)/Corn Starch Biodegradable Composite

Tsutomu Ohkita, Seung-Hwan Lee

GreenBio Institute, 15 Shimogamo Morimotocho, Sakyoku, Kyoto 606-0805, Japan

Received 12 April 2004; accepted 23 September 2004
DOI 10.1002/app.21741
Published online in Wiley InterScience (www.interscience.wiley.com).

ABSTRACT: The effects of corn starch (CS) filler and lysine diisocyanate (LDI) as a coupling agent on the crystallization behavior of a poly(butylene succinate) (PBS)/CS ecocomposite were investigated using differential scanning calorimetry. In isothermal crystallization, n values for pure PBS were from 2.33 to 2.82. On the other hand, both composites showed values of $3 < n < 4$. In nonisothermal crystallization, the Avrami exponent varied from 2.12 to 2.55 for pure PBS, from 1.58 to 1.96 for the composite without LDI, and from 1.79 to 1.91 for the composite with LDI, depending on the cooling rate. There was not a large difference of the crystallization rate constant (k) as adjusted by the Jeziornay suggestion. The activation energy for nonisothermal crystallization was also calculated on the basis of three different equations (Augis–Bennett, Kissinger, and Takhor equations). However, the values of the activation energy were in contradiction with the results of the kinetics. The addition of the filler (CS) and coupling agent (LDI) affected the morphological structure of PBS spherulites. © 2005 Wiley Periodicals, Inc. J Appl Polym Sci 97: 1107–1114, 2005

Key words: crystallization behavior; poly(butylene succinate); corn starch; composite

INTRODUCTION

The development of biodegradable-polymer natural resource composites has attracted much attention in order to solve the environmental pollution that is due to synthetic plastics waste, to effectively utilize bio-based renewable resources, and to avoid the massive usage of limited petroleum resources.

From these backgrounds, we have developed ecocomposites from poly(butylene succinate) (PBS) and corn starch (CS) by a reactive melting process using lysine diisocyanate (LDI) as a coupling agent.[1] PBS is one of the most popular biodegradable polymers and it is a semicrystalline polymer. Its chemical structure is shown below:

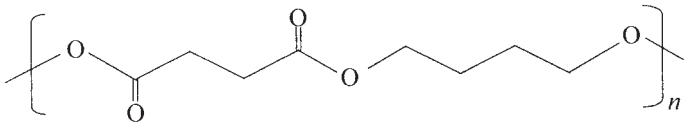

It can be very easily biodegraded in soil and by enzymes.[2,3] Starch, which can be obtained from various botanical sources, is one of the most abundant natural polymers on the earth. Its application as a filler for polymer matrix composites has been actively performed because of its excellent biodegradability, low cost, and good reinforcing effect.[4–12] LDI used as coupling agent is a lysine-based DI and it is expected to produce polyurethane, which does not yield toxic degradation products during degradation. Lysine is one of the amino acids.[13] It was found in our previous study that the tensile properties and water resistance of PBS/CS composites were improved, and these improvements were due to the improved interfacial adhesion between the polymer matrix and CS by the coupling effect of LDI. Furthermore, a sufficient effect as a coupling agent was obtained even by the addition of very small amount (<1 wt %) of isocyanates.[1]

In this study we investigated the effects of CS filler and LDI as a coupling agent on the crystallization behavior of PBS/CS biocomposites.

EXPERIMENTAL

Materials

PBS (Enpol G5300) was purchased from Ire Chemical Ltd. (Wonju, Korea), and CS (28% amylose content) was kindly supplied by Sanwa Cornstarch Co., Ltd.

Correspondence to: S.-H. Lee (Lshyhk@hotmail.com).

(Nara, Japan). CS was oven dried at 105°C for 6 h, and PBS was vacuum dried at 40°C for 24 h before use. LDI was kindly supplied by Kyowa Hakko Co., Ltd. (Tokyo). All other chemicals were purchased from commercial sources.

DSC measurements

The DSC measurements were performed on a Perkin–Elmer DSC-7 differential scanning calorimeter. For isothermal crystallization, each hot-pressed sample was first heated to 150°C and kept for 5 min to eliminate the thermal history. Then, it was rapidly cooled to a certain temperature (90–102.5°C), isothermally crystallized for a certain time, and reheated to 150°C at a rate of 20°C/min.

To examine the nonisothermal crystallization kinetics, after heating, the samples were cooled to 40°C at rates of 10, 20, 30, and 40°C/min and then reheated to 150°C at 20°C/min. The exothermic peak of the cooling curves and the endothermic peak of the reheating curves were termed the crystallization temperature (T_c) and melting temperature (T_m), respectively.

Polarizing microscope

The morphologies of the spherulites of pure PBS and PBS/CS composites with and without LDI were observed with a polarizing microscope (Olympus BH-2). Each sample was placed on a hot stage (Japan HIGHTECH Co., LK-600PM), melted at 150°C, and kept for 5 min to remove the memory of previous thermal and mechanical histories. When cooling it at a rate of 10°C/min, the spherulite growth was observed.

RESULTS AND DISCUSSION

Isothermal kinetics

Pure PBS and the PBS/CS (90/10) composites with and without LDI were isothermally crystallized at 80–100, 92.5–100, and 95–102.5°C from the melt, respectively. Generally, isothermal crystallization kinetics can be examined using the Avrami equation:

$$1 - X(t) = \exp(-kt^n) \quad T = \text{constant} \qquad (1)$$

where t is time, k is the crystallization rate constant, and n is the Avrami exponent. The relative degree of crystallinity [$X(t)$] was calculated by the following equation:

$$\int_{t_o}^{t} (dH/dt)dt \Big/ \int_{t_o}^{t_\infty} (dH/dt)dt \qquad (2)$$

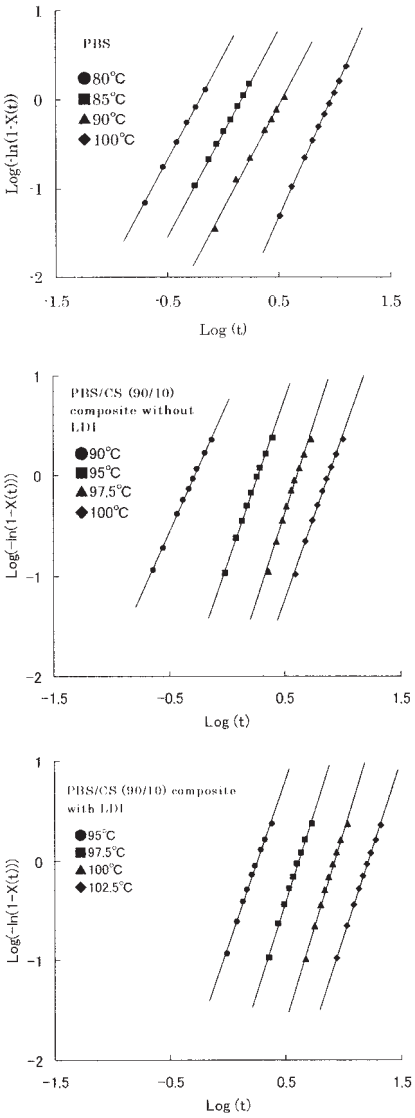

Figure 1 Avrami plots of log[1 − ln(1 − $X(t)$)] versus log t of pure PBS and the PBS/CS (90/10) composites with and without LDI.

where t_0 and t_∞ are the crystallization onset and end time, respectively.

Equation (1) can be rewritten as follows:

$$\log[1 - \ln(1 - X(t))] = \log K + \text{n} \log t \qquad (3)$$

Figure 1 shows the Avrami plots of log[1 − ln(1 − $X(t)$)] versus log t. The obtained Avrami exponents (n) are summarized in Table I.

The exponent n is assumed to indicate the type of nucleation and dimensionality of crystal growth. That is, in homogeneous nucleation, $n = 2$ theoretically means 1-dimensional (1D) growth, $n = 3$ is 2D growth, and $n = 4$ is 3D growth. In heterogeneous nucleation, $n = 1$ means 1D growth, $n = 2$ is 2D growth, and $n = 3$ is 3D growth.

TABLE I
Avrami Exponents (*n*) at Various Crystallization Temperatures for Pure PBS and PBS/CS (90/10) Composites with and without LDI

	Avrami exponent (*n*)		
Temp. (°C)	PBS	PBS/CS (90/10) without LDI	PBS/CS (90/10) with LDI
102.5	—	—	3.55
100	2.81	3.26	3.78
97.5	—	3.56	3.60
95	—	3.30	3.36
90	2.35	2.55	—
85	2.34	—	—
80	2.33	—	—

For pure PBS, the n values were from 2.33 to 2.82. These values were somewhat confusing because the PBS crystal shows spherulitic growth (3D). However, other literature data show such experimental results, and the cause is not clear at present.[14–17].

In contrast, both composites showed values of $3 < n < 4$, which are obviously larger than that of pure PBS. This suggests that there is no limitation of the crystal growth direction in isothermal crystallization. Generally, nucleation and crystal growth are more complicated in the case of the composite, because the filler can play the role of a nucleation agent or limit the normal crystal growth in certain area. Thus, the Avrami exponents of the composites should be thought of as complicated values in the two component composites.

Nonisothermal crystallization

An understanding of nonisothermal crystallization behavior is of great importance, because most processing techniques are actually conducted under nonisothermal conditions.

Figure 2 shows the crystallization exotherms of pure PBS and PBS/CS (90/10) composites with and without LDI for nonisothermal crystallization from the melt at four different cooling rates ranging from 10 to 40°C/min. When the cooling rate increased, the exotherms became broader and shifted to the lower temperature. Table II summarizes the values of the nonisothermal crystallization temperatures (T_c) and the crystallization enthalpies (ΔH_c). The T_c values of the composites were higher than that of pure PBS at the same cooling rate. Therefore, it can be said that the CS in PBS is a nucleating agent in nonisothermal crystallization. Furthermore, the composite with LDI showed a higher T_c than the composite without LDI, indicating that the crystallization rate was further increased by the addition of LDI. Conversely, the ΔH_c values of the composites with LDI were slightly lower than those of the composite without LDI at the same

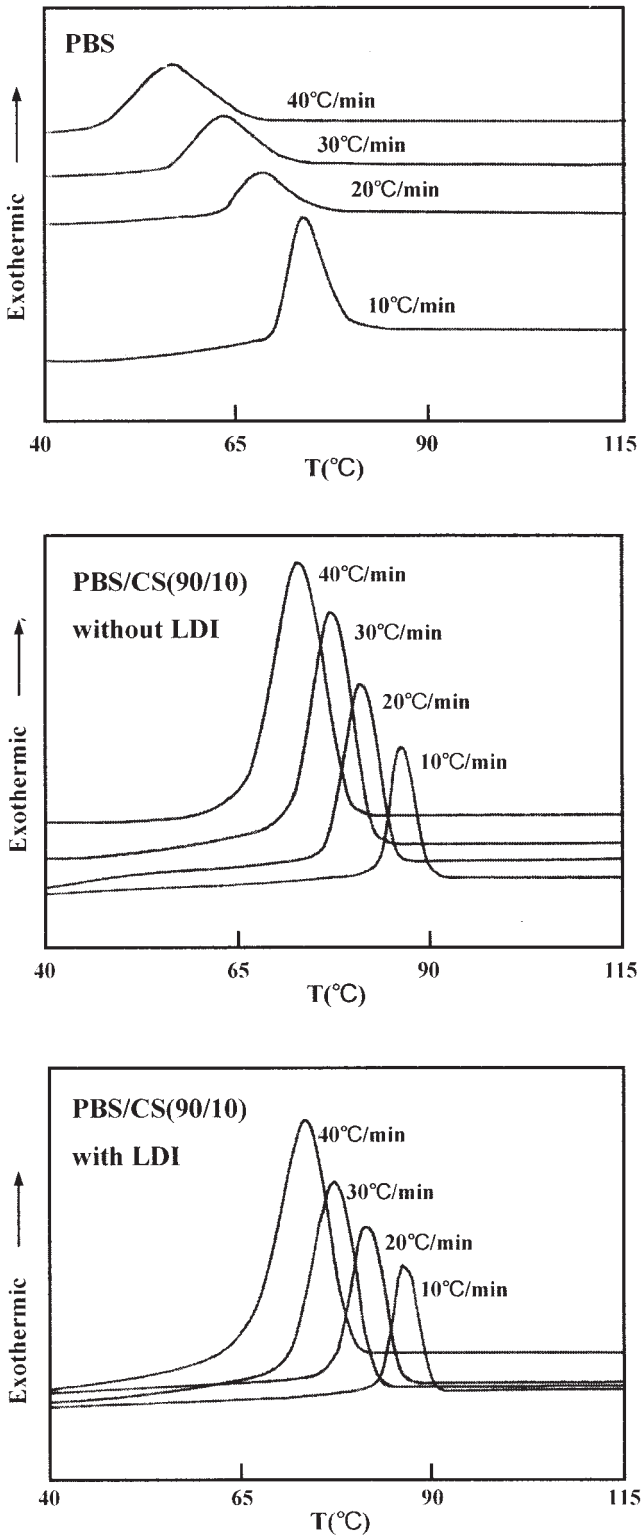

Figure 2 The crystallization exotherms of pure PBS and PBS/CS (90/10) composites with and without LDI for nonisothermal crystallization from the melt at four different cooling rates ranging from 10 to 40°C/min.

TABLE II
Crystallization Temperatures (T_c) and Enthalpies (ΔH_c) for Pure PBS and PBS/CS (90/10) Composites with and without LDI at Various Cooling Rates (γ)

Sample	γ (°C/min)	T_c (°C)	ΔH_c (J/g)
PBS	10	73.74	60.92
	20	68.08	60.13
	30	62.99	56.79
	40	56.25	56.24
PBS/CS (90/10) without LDI	10	83.37	52.89
	20	81.56	53.08
	30	77.82	53.50
	40	73.56	53.00
PBS/CS (90/10) with LDI	10	86.44	49.95
	20	81.66	51.12
	30	77.94	52.05
	40	73.63	51.81

cooling rate. This means that the crosslinking attributable to LDI may make it difficult to move the PBS molecules, restricting the folding of the molecule chains.

From the exothermic peaks of each sample, the relative degree of crystallinity [$X(T)$] was calculated by the following equation:

$$\int_{T_o}^{T} (dH/dT)dT \Big/ \int_{T_o}^{T_\infty} (dH/dT)dT \tag{4}$$

where T_0 and T_∞ are the onset and end crystallization temperatures, respectively; and dH is the enthalpy of crystallization released during an infinitesimal temperature range dT.

Figure 3 shows the plot of $X(T)$ versus the crystallization temperature (T) of each sample at different cooling rates. This temperature scale can be changed into a time scale by using the following relationship:

$$t = (T_0 - T)/\gamma \tag{5}$$

where T is the temperature at crystallization time t and γ is the cooling rate.

Figure 4 shows the plots of the $X(t)$ as a function of time for pure PBS and the composites with and without LDI. Thus, the Avrami plots of $\log[1 - \ln(1 - X(t))]$ versus $\log(t)$ at different cooling rates can be plotted as shown in Figure 5. The half-crystallization time and Avrami exponent were obtained from Figures 4 and 5, respectively, and these values are summarized in Table III. However, the crystallization rate constant of the Avrami equation should be corrected, because the temperature changes instantly in nonisothermal crystallization.[18,19] The crystallization rate constant of nonisothermal crystallization can be adequately adjusted by the following equation:

$$\log k_{non} = (\log k)/\gamma \tag{6}$$

where k_{non} is the crystallization rate constant in nonisothermal crystallization.

The adjusted values are also summarized in Table III. In all samples, when the cooling rate increased, the half-crystallization time decreased. Both composites showed shorter times than pure PBS at the same cooling rate, but there was no significant difference between both composites with and without LDI.

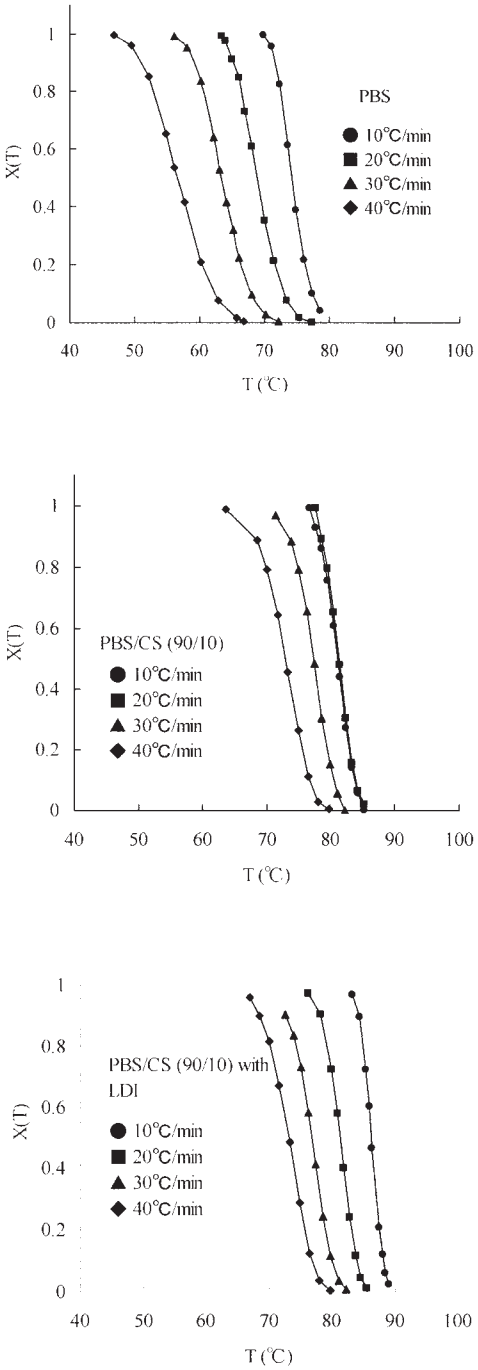

Figure 3 The plot of $X(T)$ versus the crystallization temperature (T) of each sample at different cooling rates.

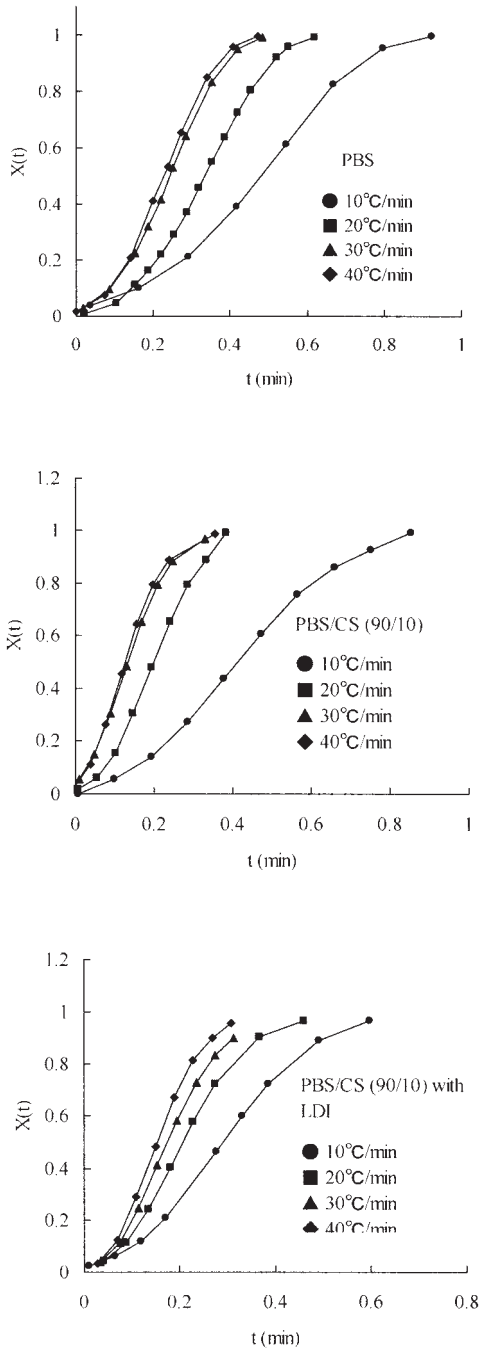

Figure 4 The plots of the relative degree of crystallinity [$X(t)$] as a function of time, which is converted from the relationship of the temperature and cooling rate for pure PBS and the composites with and without LDI.

For the nonisothermal melt crystallization, the Avrami exponent varied from 2.12 to 2.55 for pure PBS, from 1.58 to 1.96 for the composite without LDI, and from 1.79 to 1.91 for the composite with LDI, depending on the cooling rate. At all cooling rates, the Avrami exponent of all samples did not show large differences, indicating the nucleation mechanism and crystal growth geometries are similar regardless of changing the cooling rate. As compared to isothermal crystallization, in the case of pure PBS, the values were similar to those of isothermal crystallization. However, the values of both composites were smaller than those of isothermal crystallization. Furthermore, the values were obviously smaller than those of pure PBS. This decrease assumes that the crystallization growth of PBS in the composites was more limited in noniso-

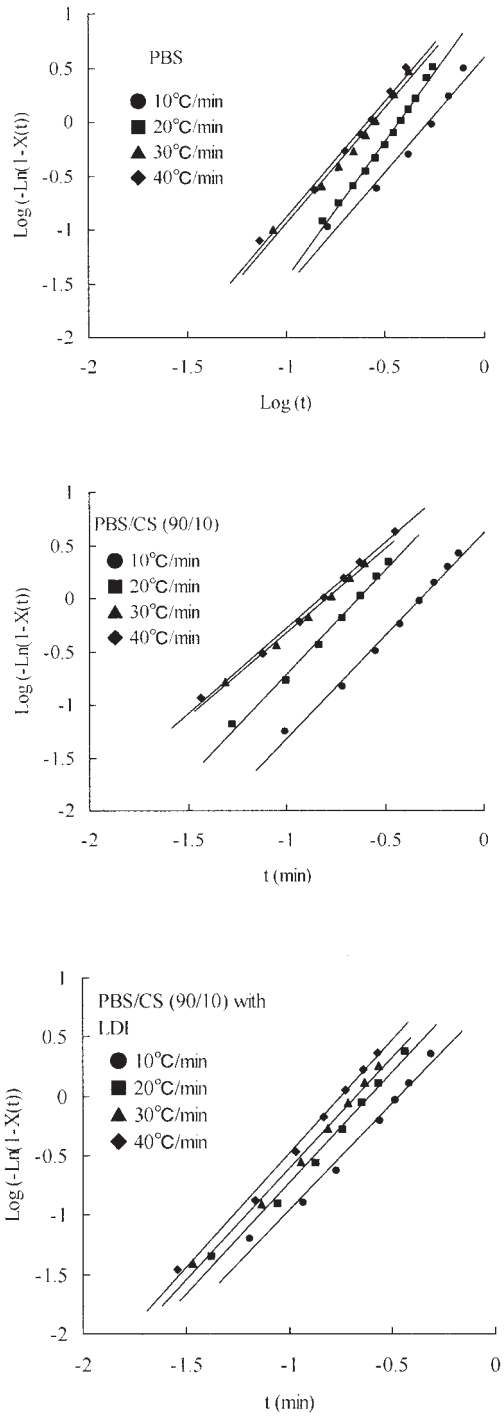

Figure 5 The Avrami plots of $\log[1 - \ln(1 - X(t))]$ versus $\log t$ at different cooling rates.

TABLE III
Half-Crystallization Time ($t_{1/2}$), Avrami Exponent (n), and Corrected Crystallization Rate Constant (k_{non}) at Different Cooling Rates for Pure PBS and PBS/CS (90/10) Composites with and without LDI

Sample	γ (°C/min)	$t_{1/2}$ (min)	n	k_{non} (min^{-n})
PBS	10	0.48	2.12	1.37
	20	0.34	2.55	1.13
	30	0.24	2.14	1.09
	40	0.23	2.15	1.07
PBS/CS (90/10) without LDI	10	0.41	1.93	1.15
	20	0.20	1.96	1.15
	30	0.13	1.58	1.09
	40	0.12	1.61	1.07
PBS/CS (90/10) with LDI	10	0.29	1.91	1.22
	20	0.20	1.79	1.13
	30	0.16	1.87	1.11
	40	0.14	1.86	1.09

thermal crystallization, in which the temperature is instantly changing, than in isothermal crystallization, in which the temperature is constant. There was not a large difference in the adjusted crystallization rate constant (k) in all samples.

Activation energy for crystallization

The activation energy for nonisothermal crystallization can be obtained following the Augis–Bennett equation,[20]

$$d[\ln(\gamma/(T_0 - T))]/d(1/T) = -E/R, \quad (7)$$

the Kissinger equation,[21]

$$d[\ln(\gamma/(T^2))]/d(1/T) = -E/R, \quad (8)$$

and the Takhor equation,[22]

$$d[\ln(\gamma)]/d(1/T) = -E/R, \quad (9)$$

where T_0 is an initial temperature and T is a peak temperature.

Figure 6 shows the plots based on Augis–Bennett,[20] Kissinger,[21] and Takhor[22] equations in nonisothermal crystallization. From the slope, the E values of all samples were calculated and are summarized in Table IV.

The absolute E value of both composites was larger than that of pure PBS, indicating that the composite required more energy to crystallize in nonisothermal crystallization. However, this result is in contradiction with the results mentioned above. That is, the nucleation of the composites was easier than that of pure PBS. Thus, these values of activation energy have to be adjusted and do not have the same physical meaning as the general activation energy. Wang et al. reported the same conclusion as our results.[18] They investigated the activation energy for the nonisothermal

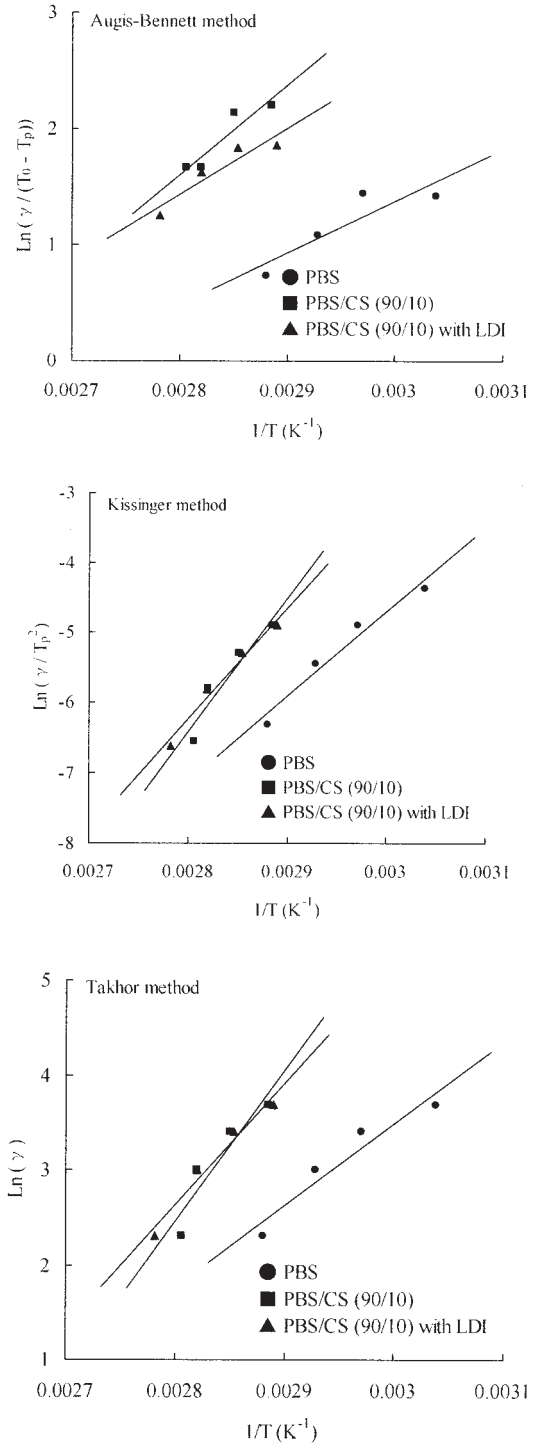

Figure 6 The determination of the activation energy describing the nonisothermal crystallization process for PBS and PBS/CS (90/10) composites with and without LDI.

TABLE IV
Activation Energy for Crystallization of Pure PBS and PBS/CS (90/10) Composites with and without LDI

Sample	*E* (kJ/mol)		
	Augis–Bennett equation	Kissinger equation	Takhor equation
PBS	−37.41	−101.16	−71.79
PBS/CS (90/10)	−63.85	−158.34	−132.13
PBS/CS (90/10) with LDI	−47.35	−131.95	−105.96

crystallization of pure poly(ethylene terephthalate) (PET) and PET/clay nanocomposites and concluded that the values of the activation energy are just adjustable parameters because the nanocomposite crystallizes faster than PET, whereas the activation energy was higher than pure PET.

Crystalline morphology

The introduction of the filler (CS) and coupling agent (LDI) will influence the morphological structures of the PBS crystal such as spherulite size, shape, and nucleation density. Figures 7–9 show the crystalline growth of pure PBS and PBS/CS (90/10) composites without and with LDI, respectively.

The spherulites of pure PBS grew over 20 μm at 81.9°C and the shape was a clear round. However, the composites without and with LDI started to crystallize at 91.4 and 92.5°C, respectively. That is, the crystallization rate was faster in the order of the composite with LDI > the composite without LDI > pure PBS. This result agreed with the results of the DSC. Furthermore, the addition of CS decreased the size of the spherulites and the shape of the spherulites was irregular. In both composites, the interfaces of the spherulites were blurry and the nucleation density was higher than pure PBS.

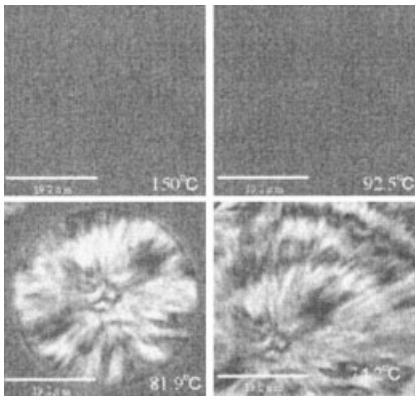

Figure 7 The spherulite growth appearance of pure PBS.

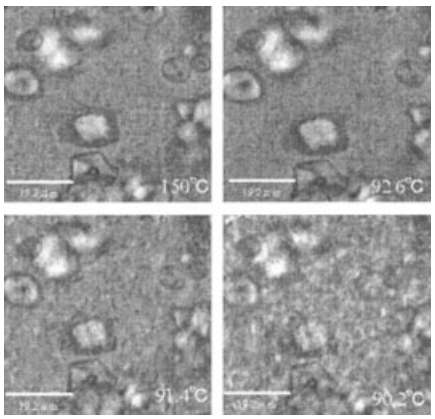

Figure 8 The spherulite growth appearance of the PBS/CS (90/10) composite without LDI.

CONCLUSION

In isothermal crystallization, the n values for pure PBS were from 2.33 to 2.82. In contrast, both composites showed values of $3 < n < 4$, suggesting that there is no limitation of the crystal growth direction in isothermal crystallization. In nonisothermal crystallization, the Avrami exponent varied from 2.12 to 2.55 for pure PBS, from 1.58 to 1.96 for the composite without LDI, and from 1.79 to 1.91 for the composite with LDI, depending on the cooling rate. These smaller values in both composites assumed that the crystallization growth or nucleation of PBS in the composites was more limited or faster in nonisothermal crystallization, respectively. There were no large differences in the crystallization rate constant adjusted by the Jeziornay[19] suggestion. The activation energy for nonisothermal crystallization was calculated on the basis of three different equations. However, the values of the activation energy were in contradiction with the results of the kinetics. The addition of CS and LDI affected the morphological structure of PBS spherulites, decreasing the size of

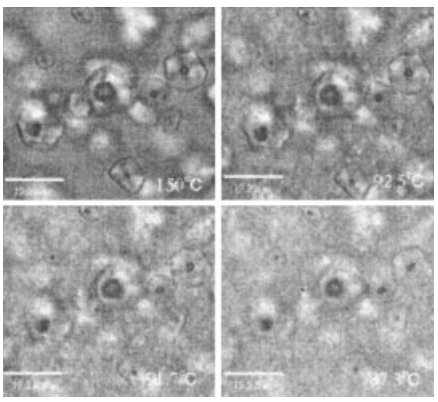

Figure 9 The spherulite growth appearance of the PBS/CS (90/10) composite without LDI.

the spherulites and making the shape of the spherulites irregular.

References

1. Ohkita, T.; Lee, S. H. J Adhes Sci Technol 2004, 18, 905.
2. Honda, N.; Taniguchi, I.; Miyamoto, M.; Kimura, Y. Macromol Biosci 2003, 3, 189.
3. Lee, S. H.; Ohkita, T.; Kimura, A. Polym Prepr 2003, 52, 1091.
4. Ke, T.; Sun, X. Cereal Chem 2000, 77, 761.
5. Ke, T.; Sun, X. Trans ASAE 2001, 44, 945.
6. Ke, T.; Sun, X. J Appl Polym Sci 2001, 81, 3069.
7. Thiebaud, S.; Aburto, J.; Alric, I.; Borredon, E.; Bikiaris, D.; Prinos, J.; Panayiotou, C. J Appl Polym Sci 1997, 65, 705.
8. Vega, D.; Villar, M. A.; Failla, M. D.; Valles, E. M. Polym Bull 1996, 37, 229.
9. Shogren, R. L.; Thompson, A. R.; Felker, F. C.; Harry-Okuru, R. E.; Gordon, S. H.; Greene, R. V.; Gould, J. M. J Appl Polym Sci 1992, 44, 1971.
10. Yavuz, H.; Babac, C. J Polym Environ 2003, 11, 107.
11. Liu, W.; Wang, Y.-J.; Sun, Z. J Appl Polym Sci 2003, 88, 2904.
12. Wu, C. S. J Appl Polym Sci 2003, 89, 2888.
13. Yamaguchi, T.; Otsuka, H.; Takahara, A. Polym Prepr 2003, 52, 3945.
14. Nishio, Y.; Hirose, N.; Takahashi, T. Seni Gakkaishi 1990, 46, 441.
15. Calaahorra, E.; Cortazar, M.; Guzman, G. M. Polym Commun 1983, 24, 211.
16. Martuscelli, E.; Silvestre, C.; Gismondi, C. Makromol Chem 1985, 186, 2161.
17. Katime, I. A.; Anasagasti, M. S.; Peleteiro, M. C.; Valenciano, R. Eur Polym J 1987, 23, 907.
18. Wang, Y.; Shen, C.; Li, H.; Li, O.; Chen, J. J Appl Polym Sci 2004, 91, 308.
19. Jeziornay, A. Polymer 1978, 19, 1142.
20. Augis, J. A.; Bennett, J. E. J Thermal Anal 1978, 13, 283.
21. Kissinger, H. E. J Res Natl Bur Stand 1956, 57, 217.
22. Takhor, R. L. Advances in Nucleation and Crystallization of Glasses; American Ceramics Society: Columbus, OH, 1971; p 166.